

## **Scope of Work For**

### **Project 14-014**

# **Constraining NO<sub>x</sub> Emissions Using Satellite NO<sub>2</sub> Column Measurements over the Southeast Texas**

Prepared for

Air Quality Research Program (AQRP)  
The University of Texas at Austin

#### **PREPARED BY**

University of Houston  
4800 Calhoun Road  
Houston, Texas 77204-5007

*Principal Investigator*  
Yunsoo Choi

*Co-PI*  
Xiangshang Li

December, 2014

## 1. Background

Previous studies in our group focused on showing the impact of lightning and/or anthropogenic sources on tropospheric concentrations of nitrogen oxide ( $\text{NO}_x$ ) and ozone ( $\text{O}_3$ ) over the continental United States for summer 2005 (e.g., Choi et al., 2005, 2008a, 2008b, 2009) and summer 2009 (e.g., Choi et al., 2012; Choi, 2013). Multi-year trends in observed surface concentrations of  $\text{NO}_x$  and  $\text{O}_3$  are the result of the changes in the natural and anthropogenic sources (e.g., emission changes). One of the previous studies was performed by utilizing satellite products to estimate the posteriori emissions for surface  $\text{NO}_x$  emissions (e.g., Choi et al., 2008a).

Biogenic Volatile Organic Compound (VOC) emissions are temperature (T) and solar radiation dependent (Guenther et al., 1995). High temperatures enhance biogenic isoprene emissions, leading to increased production of carbon monoxide (CO) and formaldehyde (HCHO) (e.g., Atkinson and Arey, 1998; Guenther et al., 1999; Palmer et al., 2003; Millet et al., 2006). The oxidation process of short-lived biogenic VOCs (e.g., Sharkey et al., 1999; Pfister et al., 2008) affects the distribution of HCHO and CO over the US (e.g., Hudman et al., 2009; Choi et al., 2010). In this proposal, we will evaluate the concentrations of isoprene and HCHO using the measurements from the Deriving Information on Surface conditions from Column and Vertically Resolved Observations Relevant to Air Quality (DISCOVER-AQ) Houston aircraft project and the nitric oxide ( $\text{NO}_2$ )/HCHO ratio over southeast Texas.

The changes in  $\text{NO}_x$  also affect the atmospheric chemical environment, resulting in the change of  $\text{NO}_x$ /VOC ratios over Southeast Texas. The  $\text{NO}_x$ /VOC ratio affects the chemical regime and thus the production rate of  $\text{O}_3$  (e.g., Martin et al., 2004; Duncan et al., 2010; Choi et al., 2012) and the weekly cycles of surface  $\text{O}_3$  as shown in our previous study by Choi et al. (2012). In this project, we will investigate  $\text{NO}_x$ /VOC ratio changes as  $\text{NO}_x$  emissions change. Particularly, in order to investigate the sensitivities of the production efficiencies of tropospheric  $\text{O}_3$  (e.g., Global Ozone Monitoring Experiment-2 (GOME-2) and/or *Ozone Monitoring Instrument* (OMI)), the remote sensing  $\text{NO}_2$ /HCHO ratio (e.g., Choi et al., 2012, Choi, 2014), will be utilized to represent the atmospheric environment for the DISCOVER-AQ time periods.

In our previous studies, we separated the continental US into six different geographical regions to analyze the uncertainty of anthropogenic  $\text{NO}_x$  emissions modified from the National Emission Inventory 2005 (NEI2005) using the Community Air Quality Model (CMAQ) v4.7.1 with a 12km resolution (the  $\text{NO}_x$  emission reductions of point sources were considered from 2005 to 2009, called as “EMIS2009”, Choi et al., 2012). From GOME-2  $\text{NO}_2$  retrievals for August 2009, we calculated monthly-averaged concentrations of the  $\text{NO}_2$  column. For comparison to model output, we will re-grid the  $\text{NO}_2$  column data to our model grid. We also estimated monthly column values of  $\text{NO}_2$  concentrations from the model with EMIS2009. We performed an additional simulation, including remote sensing-adjusted  $\text{NO}_x$  anthropogenic source emissions (e.g., Choi et al., 2008a; Choi et al., 2012). The GOME-2 adjusted  $\text{NO}_x$  emissions (426 Gg N) (called as “EMISGOME”) were found to be 7.8% less than EMIS2009 (462 Gg N) over the US (Choi et al., 2012). Observed and model-simulated  $\text{NO}_x$  concentrations at the AQS stations over the geographical regions were estimated. We found that for the Pacific Coast (PC), Rocky Mountain (RM), Lower Middle (LM), Upper Middle (UM), South East (SE), and North East (NE) regions, with relatively high correlation coefficients among hourly  $\text{NO}_x$  data from

observations and two CMAQ model runs ( $R > 0.7$ ), the biases of baseline model are generally; the biases of model, including emissions changes, improve in terms of absolute amount of normalized mean bias except for RM (Choi, 2014). Interestingly, among six geographical regions, the noticeable changes in biases are found over LM in US, reducing NMB from +149.7% to -1.8%. Over LM, a significantly large reduction in  $\text{NO}_x$  biases suggests that the  $\text{NO}_x$  emissions from EMIS2009 were probably too high.

The zoomed-in regionalized studies were performed over Houston to highlight the uncertainties of EMIS2009 emissions from the previous study (Choi, 2014). The model with EMISGOME mitigated the discrepancies between simulated and observed surface  $\text{NO}_x$  over Houston. The large  $\text{NO}_x$  emissions-reduction decreases surface  $\text{NO}_x$  concentrations over Houston, which mitigates the discrepancy between surface  $\text{NO}_x$  concentrations of model and observation. This investigation will be performed in the urban areas of the Southeast Texas for the time period of DISCOVER-AQ Houston. In order to perform this analysis, we will re-estimate the posteriori emissions using an inverse method with remote sensing data (Shim et al., 2005) and/or EPA national emission trends (Czader et al., 2014) to consider error uncertainties from modeling and remote sensing. We will also examine how posteriori  $\text{NO}_x$  emissions affect modeling biases over the Southeast Texas.

In addition to the  $\text{NO}_x$  and VOC emissions, many studies (e.g. Banta et al., 2005; Ngan et al., 2012), pointed out the importance of meteorological processes on air quality. To improve the meteorological simulation, we will adopt an objective analysis (OA) process to assimilate point observational data in order to reduce the uncertainties in Weather and Research Forecasting (WRF) (Skamarock et al., 2008) simulation. Using a state-of-the-art meteorological model such as WRF, along with the adoption of OA, should provide an optimal meteorological simulation. OA improves the meteorological analyses of coarse resolution on the model grid by incorporating information from in-situ observations. Without local information, the simulated meteorology (especially the wind fields) may deviate markedly from reality. OA has been shown to be very effective to rectify the model's surface level wind, a parameter critical to the overall model performance (e.g. Ngan et al., 2012, Li et al 2014) and to improve air quality modeling (Czader et al., 2013).

## **2.0 Statement of Work**

### **2.1 Objectives of the Present Study**

The overall objective of the present study is to address the  $\text{NO}_x$  emissions issues in the current EPA emission inventory discussed above. To accomplish this, we will analyze ambient  $\text{NO}_x$  data from P3-B aircraft campaign over the greater Houston area in the September of 2013 during the Deriving Information on Surface Conditions from the Column and Vertically Resolved Observations Relevant to Air Quality (DISCOVER-AQ) and column data from OMI satellite. Then we will apply inverse modeling to derive posteriori emissions for the  $\text{NO}_x$ . In addition, we will analyze the  $\text{NO}_x$  and HCHO performance, as well as impact on ozone using posteriori emissions adjusted for the  $\text{NO}_x$ .

Our main objectives are:

- 1) Quantify the posteriori  $\text{NO}_x$  emissions from a priori surface emission sources (e.g., point, area, mobile, area, and soil sources) using an inverse method with satellite  $\text{NO}_2$  columns.
- 2) Evaluate model-simulated HCHO and isoprene concentrations using in-situ ground and/or aircraft measurements.
- 3) Examine how the monthly averaged ratios of  $\text{NO}_2$  /HCHO vary spatially.
- 4) Additionally, examine how the in-situ measurement adjusted meteorology improves the meteorological and photochemical model predictions.

## 2.2 Specific Implementation Tasks

### 1. WRF and CMAQ model runs (Dr. Xiangshang Li and Ph.D. student, Lijun Diao)

The WRF and CMAQ simulation period is selected to be **September 2013**, the DISCOVER-AQ 2013 intensive field campaign period.

#### 1.1 WRF runs

##### i. Domain setup

The WRF domains have sizes of  $161 \times 145$  for the 12-km domain, and  $97 \times 79$  for the 4-km domain. WRF domains are shown in Figure 1, as red and blue boxes.

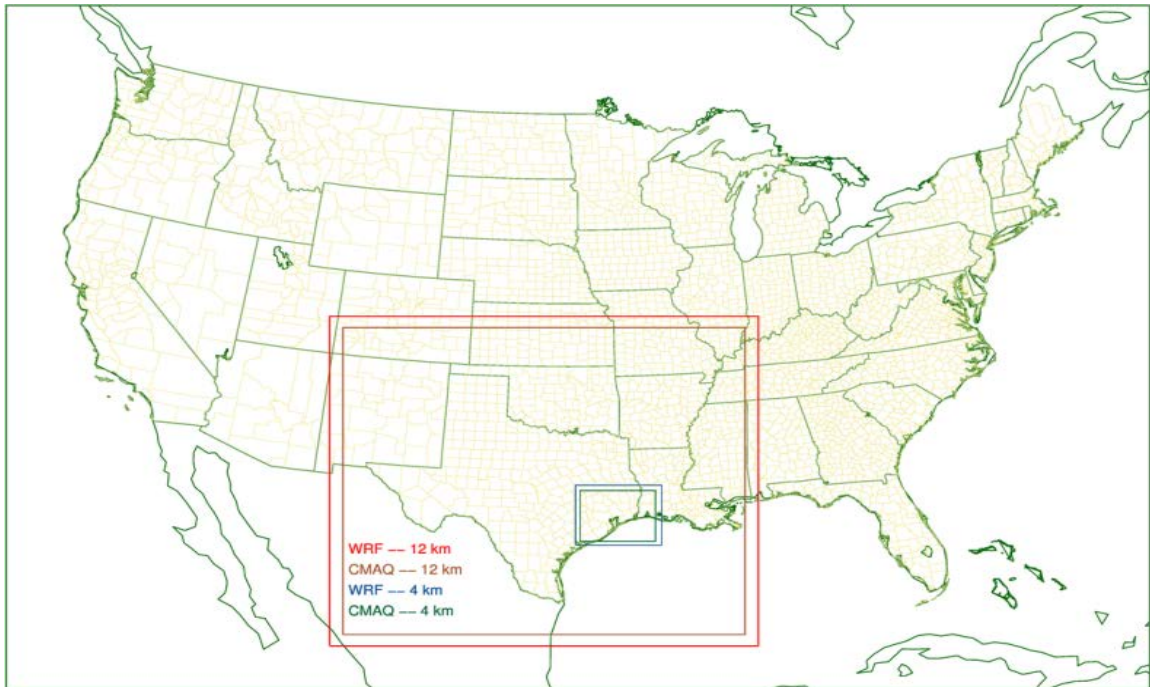


**Figure 1:** WRF (thick lines) and CMAQ (thin lines) used for the UH Air Quality Forecasting (AQF) System. There are two domains: the 12-km Texas domain and the 4-km Houston-Galveston-Brazoria (HGB) domain.

Both WRF and CMAQ share the same vertical structure since no layer collapsing has been employed in Meteorology-Chemistry Interface Processor (MCIP). The vertical structure is listed in Table 1.

Layer	AGL(m)	Layer	AGL(m)
1	32.4	15	1517.8
2	81.2	16	1751.4
3	163.1	17	1990
4	245.9	18	2233.9
5	329.5	19	2534.7
6	413.7	20	3164.8
7	498.4	21	4193.1
8	583.8	22	5415.3
9	669.7	23	6964.2
10	756.2	24	9083.3
11	887.2	25	11444.6
12	1019.6	26	14549.2
13	1153.4	27	16540.7
14	1288.8		

**Table 1:** Vertical layer structures of WRF and CMAQ used for the modeling

**ii. Input analysis data for WRF**

We have evaluated existing analysis datasets and decided to use North American Regional Reanalysis (NARR) as input. The NARR data are based on an Eta 221 grid at 29 pressure levels. Its horizontal resolution is 32-km and the frequency is 3-hourly. An alternative to NARR is the Eta- North American Mesoscale Model (NAM) analysis data. However, the data frequency was lowered from every three hour to every six hours starting in 2013. Our test showed Eta-NAM analysis is not as good as NARR for WRF input.

**iii. Proposed major WRF configurations**

Proposed WRF options are shown in Table 2 below. The first guess and boundary conditions will be generated by WRF-real from the NARR analyses. The grid nudging is turned on with the same NARR analysis data.

WRF Version	V3.6.1, latest
Microphysics	Lin et al. Scheme
Long-wave Radiation	Rapid Radiative Transfer Model for GCMs (RRTMG)
Short-wave Radiation	New Goddard scheme
Surface Layer Option	Monin-Obukhov with Carslon-Boland viscous sublayer scheme
Land-Surface Option	Unified Noah LSM (Land Surface Model)
Urban Physics	None
Boundary Layer Scheme	Yonsei University (YSU)
Cumulus Cloud Option	Kain-Fritsch
Four Dimensional Data Assimilation	Grid and observation-nudging

**Table 2:** WRF physics options

#### **iv. Nudging (grid, surface and observation nudging)**

Observational nudging is regarded as a low-cost and effective method in improving meteorological model performance, but it requires additional observational data. In this study, we acquire the input observation data and generating files in little\_r format using UH in-house developed codes. Observational data come from the Meteorological Assimilation Data Ingest System (MADIS) and Continuous Ambient Monitoring Station (CAMS). MADIS is a National Oceanic and Atmospheric Administration (NOAA) program that collects, integrates, checks for quality, and distributes observations from NOAA and non-NOAA organizations. The four MADIS datasets used for the obs-nudging are NOAA Profiler Network (NPN), Cooperative Agency Profilers (CAP), Aviation Routine Weather Report (METAR) and NOAA Radiosonde (RAOB). CAMS is a surface based monitor network measuring pollutants, nutrients, or other parameters. It is maintained by Texas Commission on Environmental Quality (TCEQ).

Most of the observation data are available in hourly frequency. Therefore, we plan to implement hourly observation nudging. The key settings in WRF for hourly observational nudging are “intf4d” in “namelist.ou”, and “auxinput11\_interval”, “sgfdda\_interval\_m” in “namelist.input”.

### **1.2 CMAQ runs with 2011 National Emission Inventory**

#### **i. Domain setup**

We expect that the CMAQ modeling domain will be, 150×134 cells at 12-km, and 84×66 cells at 4-km domains, respectively.

The CMAQ domains are also shown in Figure 1, as brown and green boxes.

#### **ii. Emission processing**

Model-ready emissions are to be prepared using the Sparse Matrix Operator Kernel Emissions (SMOKE) model. For emission inventory other than mobile sources, we will use the 2011 National Emission Inventory (NEI2011) generated by the Environmental Protection Agency (EPA) or latest Texas Emission Inventory (TEI) if either is officially

released and adapted to CMAQ. Emissions from natural sources were estimated with Biogenic Emissions Inventory System (BEIS3). The mobile emissions were processed with 2014 Motor Vehicle Emission Simulator (MOVES) using updated inventory.

There have been several significant changes made in NEI2011. Especially, on-road mobile emissions have been updated from MOVES2011 to MOVES2014. To support these changes in MOVES2014, the UH forecasting system needs to update the current SMOKE system to the latest SMOKE version 3.6 released in November 2014. Because of new Source Category Code (SCC) and activity input data updates, proper evaluation processes are required to prepare accurate emissions input files for the CMAQ modeling system.

### iii. Generating meteorological input using MCIP

Meteorological input for CMAQ will be processed using UH-modified MCIP over the WRF output. UH-modified MCIP corrected a few bugs such as a bug in layer collapsing and has minor enhancements such as improved mass-conservation formulation over the default MCIP. Traditionally, UH has contributed to the EPA MCIP code development.

### iv. Proposed major CMAQ configurations

Proposed major CMAQ configurations are shown in Table 3. All of these options have been tested by our group.

CMAQ version	V5.0.1, latest is v5.0.2
Chemical Mechanism	cb05tucl_ae5_aq: Carbon-Bond version 5 (CB05) gas-phase mechanism with active chlorine chemistry, updated toluene mechanism, fifth-generation CMAQ aerosol mechanism with sea salt, aqueous/cloud chemistry
Lightning NOx emission	Included by using inline code
Horizontal advection	Yamartino Scheme (YAMO)
Vertical advection	WRF omega formula (vwrf)
Horizontal mixing/diffusion	Multiscale (multiscale)
Vertical mixing/diffusion	Asymmetric Convective Model version 2 (acm2)
Chemistry solver	Euler Backward Iterative (EBI) optimized for the Carbon Bond-05 mechanism (ebi_cb05tucl)
Aerosol	Aerosol module version 5 (AERO5) for sea salt and thermodynamics (aero5)
Cloud Option	Asymmetric Convective Model (ACM) (cloud_acm_ae5)
Initial Condition (IC) / Boundary Condition (BC)	Default static profiles

Table 3 Major CMAQ options

### 1.3 Deliverables and expected date

A detailed report on WRF and CMAQ configurations, NEI2011 preparation and notes on the new emission inventory – expect date: March 31, 2015

## 2. Compare model to satellite NO<sub>2</sub> data (Dr. Xiangshang Li, Ph.D. student, Amir Hossein Souri)

### 2.1 General description of satellite data

NASA OMI tropospheric NO<sub>2</sub> (Level 2, V2.1) will be used for this project. Compared to Derivation of OMI tropospheric NO<sub>2</sub> (DOMINO), NASA OMI product is more consistent with validation studies (e.g., Bucsela et al., 2013). For OMI, the crossing of the equator occurs at 13:45 local time. The size of the ground footprint varies across the swath from 13×24 km<sup>2</sup> at nadir (direct from above) to ~40 ×160 km<sup>2</sup> for the edge of the orbit due to the optical aberrations and asymmetric alignment (i.e., panoramic effect). A detailed description of NO<sub>2</sub> retrieval can be found in Bucsela et al. (2013). Concisely, the acquired spectra sensed by OMI detectors are analyzed with the Differential Optical Absorption Spectroscopy (DOAS) method in a fitting window from 405 nm to 465 nm. The calculated NO<sub>2</sub> slant column densities are then corrected for instrumental defects. This is named “destriping” due to the variability of effects across the orbital track. In order to convert NO<sub>2</sub> slant column densities to vertical ones, Air Mass Factors (AMFs) which are functions of temperature, cloud cover, topography, albedo, and etc. are calculated using a pre-computed scattering-weight table from TOMS radiative transfer mode (TOMRAD) and monthly mean NO<sub>2</sub> profiles from the Global Model Initiative (GMI) simulation (here in a 2.5°×2.5° grid). The uncertainties of the product vary from location to location and under different meteorological conditions. The overall error on the tropospheric vertical column density is <30% under clear-sky conditions and typical polluted conditions (>10<sup>15</sup> molecules cm<sup>-2</sup>) (Bucsela et al., 2013).

### 2.2 Data access and data preprocessing

Daily granule (file) of tropospheric OMI NO<sub>2</sub> is available online at <http://mirador.gsfc.nasa.gov/cgi-bin/mirador/collectionlist.pl?keyword=omno2>. All the granules acquired in September of 2013 will be checked to see whether they cover Texas. This should be done, since unlike other satellites such as MODIS, there is no a fixed granule name to cover a same location in different revisits.

Three important steps in preprocessing are:

- 1) Masking pixels having low quality. The common thresholds for performing the mask are (note pixels lacking below criteria will be filtered out):  
Solar Zenith Angle (SZA)  $0 \leq \text{SZA} \leq 85^\circ$ , VCD Quality Flags=0, Root Mean Squared Error of Fit < 0.0003, Terrain Reflectivity < 30% and Cloud Fraction < 20%
- 2) Removing the vertical priori profile impact from the granules to conduct an “apple-to-apple” comparison between model and satellite.  
This will be discussed with more details in Section 2.3.
- 3) Gridding granules in high spatial resolution  
As outlined earlier, pixels located far from nadir experience very poor spatial resolution. In order to make a smooth and uniform gridding, a recent novel method

(Kuhlmann et al., 2014) will be deployed. Using the parabolic spline method in this method, NO<sub>2</sub> maps become smoother and extreme values are more accurately reconstructed. Traditionally, oversampling was the main approach to have high spatial resolution for regional analysis. This step will be used for the first time in the field of inverse modeling without oversampling.

### 2.3 Comparison with model

A direct comparison of model output to OMI NO<sub>2</sub> required that an a priori vertical profile of NO<sub>2</sub> in the OMI retrieval algorithm (here 2.5°×2.5° monthly averaged profiles from GEOS-Chem) be eliminated. Although this coarse initial guess could bias the results, the main problem lay in applying an average semi-polluted profile over the large grid cell that encompassed both urban and rural regions, resulting in an underestimation of NO<sub>2</sub> vertical columns in urban regions and an overestimation in rural regions (Russell et al., 2011). Following the approach described in Duncan et al. (2014), we will first use the variable called “scattering weight” provided for various pressure levels from the surface to the top of the atmosphere that is included in the OMI NO<sub>2</sub> data files. We will sum over all model layers the product of the scattering weight and model partial column (molecules/cm<sup>2</sup>) in each model layer (up to the tropopause pressure provided in OMI Hierarchical Data Format file). This sum divided by vertical column density of model is called the air mass factor (AMF) of the model (AMF<sub>model</sub>). Subsequently, we will divide the product of vertical column density (VCD) and AMF of satellite from the Hierarchical Data Format data file by AMF<sub>model</sub> to obtain a modified form of vertical column density of satellite though the following equation:

$$VCD'_{\text{satellite}} = (VCD_{\text{satellite}} \times AMF_{\text{satellite}}) / AMF_{\text{model}}$$

Now we can directly compare VCD' <sub>satellite</sub> to the model output. It is worth mentioning that a bilinear interpolation method will be used to co-register pixels between the satellite and model.

### 2.4 Deliverables and expected date

A detailed report on satellite data retrieval, processing and comparison to the model – expected date: April 30, 2015.

## 3. Compare model to in-situ aircraft data and surface monitors (Dr. Xiangshang Li and Ph.D. student, Lijun Diao)

### 3.1 General description of aircraft data

Aircraft measurements are available online from the NOAA aircraft P-3B, part of the datasets collected during DISCOVER-AQ campaign. The latest version of P-3B data have over 100 parameters, merged from measurements from a number of instruments on board. The data files are dated Oct. 2014. There are 10 days flight data available during the DISCOVER-AQ campaign period.

### **3.2 General description of CAMS data**

Surface observational data consist of regular measurements from CAMS, operated by the TCEQ. The CAMS measurement network collects real-time meteorology data and air pollutant concentration data. The measured parameters differ from station to station. The station density at southeast Texas is relatively high. The number of sites having meteorological, ozone and NO<sub>x</sub> measurements are 63, 52 and 30, respectively, in the 4-km domain during DISCOVER-AQ time period.

### **3.3 Data access and data preprocessing**

Aircraft data can be downloaded from DISCOVER-AQ website, which is public-accessible: <http://www-air.larc.nasa.gov/missions/discover-aq/P3B-extract.tx2013.html>. CAMS data are already archived by our group using a data-spider coded in Interactive Data Language (IDL). The data spider queries and downloads CAMS data from TCEQ website. Both the aircraft data and CAMS data are stored in text (ASCII) files, though with different format. These files need to be preprocessed into tabular forms for comparison with model data.

### **3.4 Comparison with model**

The comparison of CAMS data with model results is relatively straightforward. The first step is to extract model concentrations of NO and NO<sub>2</sub> at the surface layer. The CMAQ model outputs are binary netCDF files and we have in-house codes to extract data for any variable, and at any layer. The extracted data files are close to tabular format with headers and data section. Usually one data file is generated for each variable and each day.

To compare the model value with the observed concentration from site A, we first calculate the row and column index of site A in model grid using its latitude and longitude. For example, CAMS site 1 is located in a cell (29,29) with row number 29 and column number 29 in our 4-km domain, assuming the lower-left corner with row number 1 and column number 1 which is cell (1,1). Then we extract the model value for the grid cell and compare it to the observation. The data frequency of model output and CAMS are both hourly, making direct comparison easy.

The comparison of aircraft data with model results is more complicated since the aircraft is moving in a 3-Dimensional space. However the idea is essentially the same: to find the model data matching the location and time of aircraft point measurement. We have developed in-house codes to match model results with aircraft and ozone sonde measurements. The detailed process will be explained in a technical report. Since aircraft data have much higher frequency than model output, we will aggregate all the aircraft data points in one grid cell during 1-hour period to match model output.

### **3.5 Deliverables and expected date**

A detailed report on aircraft/CAMS data retrieval, processing and comparison to the model – expected date: May 31, 2015

#### **4. Inverse modeling (Dr. Yunsoo Choi, Ph.D. student, Amir Hossein Souri)**

##### **4.1 Setup an inverse modeling system**

We will apply a Bayesian least squares method to update the emission parameters of NO<sub>x</sub> using OMI NO<sub>2</sub>, surface and aircraft observations with CMAQ as the forward model. In the inverse model, for NO<sub>x</sub>, we will have four different emissions to consider. Nonroad emission is included in the area emission in our setup. Different observations will be used separately to update the emission inventories; additionally, a fusion way will be conducted to take into account all the observations at the same time to perform updating.

##### **4.2 Apply for the inverse model to get posteriori NO<sub>x</sub> source**

The relationship between the observation vector  $y$  (here OMI, CAMS and aircraft) and state vector  $x$  (here emissions) can be described as:

$$y = Kx + e$$

where the  $K$  matrix is a Jacobian matrix representing the NO<sub>x</sub> sensitivities to the state vector defined by CMAQ model, and  $e$  is the error term. The uncertainties will be used for weightings of the observations and the a priori state vector. Moreover, we will consider the measurement and priori model parameter errors. The a posteriori state ( $\hat{x}$ ) vector will be computed by:

$$\hat{x} = x_a + (K^T S_e^{-1} K + S_a^{-1})^{-1} K^T S_e^{-1} (y - K x_a)$$

where  $x_a$  is the a priori state vector,  $S_a$  is the estimated error covariance matrix for  $x_a$ , and  $S_e$  is the error covariance matrix for observation errors.  $K^T$  is the transpose matrix of  $K$ .

After analyzing the inverse model (e.g., ill-conditioned, freedom of Jacobian Matrix and etc.) and the error of posteriori, the updated emission inventories will be ready for the subsequent analysis.

##### **4.3 Run CMAQ with the posteriori emissions**

In order to see the impacts of updated emission inventories on ozone and NO<sub>x</sub>, the model will be simulated using the posteriori emissions. The difference of NO<sub>2</sub>/HCHO ratio between simulation using the priori and the posteriori emissions will be examined.

##### **4.4 Deliverables and expected date**

A detailed report on inverse modeling and how posteriori emissions are derived - expected date: June 30, 2015.

#### **5. Posteriori analysis of NO<sub>2</sub> and HCHO conditions (Dr. Xiangshang Li, Ph.D. student, Lijun Diao and Ph.D. student, Amir Hossein Souri)**

##### **5.1 Estimate NO<sub>2</sub>/HCHO ratio and O<sub>3</sub> impact over the Southeast Texas**

Due to uncertainties of the emission inventories, an inaccurate NO<sub>2</sub>/HCHO ratio can lead to a misunderstanding of chemical condition (NO<sub>x</sub> limited/NO<sub>x</sub> saturated) of a region. Due to different remediation for reduction in ozone and its precursors in various

chemical conditions, a precise NO<sub>2</sub>/HCHO should be observed. As a result, the improved emission inventories derived from the inverse method based on Bayesian statistics will provide a more precise picture of the chemical condition of the Southeast Texas. Using CMAQ, the changes in NO<sub>2</sub>/HCHO ratio for different emission inventories will be simulated and the resultant ozone production rate will be discussed. Further, the impact of the changes in the ratio of NO<sub>2</sub>/HCHO on the surface O<sub>3</sub> will be investigated.

## **5.2 Deliverables and expected date**

A detailed report on NO<sub>x</sub> and HCHO performance, NO<sub>2</sub>/HCHO ratio based on posteriori emissions, and changes in ozone performance- expected date: August 31, 2015.

## **2.3: Deliverables**

1. A project Work Plan, which includes a background introduction of this project, a statement of work (including goals, tasks, key personnel, deliverables, and schedule), and a budget with justification.
2. Quality Assurance Project Plan (QAPP).
3. A number of reports including quarterly and final reports will be submitted on a timely basis and at regular intervals. A description of the specific reports to be submitted and their due dates are outlined below. One report per project will be submitted (collaborators will not submit separate reports), with the exception of the Financial Status Reports (FSRs). The lead PI will submit the reports, unless that responsibility is otherwise delegated with the approval of the Project Manager. All reports will be written in third person and will follow the State of Texas accessibility requirements as set forth by the Texas State Department of Information Resources. Report templates and accessibility guidelines found on the AQRP website at <http://aqrp.ceer.utexas.edu/> will be followed.

In final report, we will include complete WRF/CMAQ model setup; observation data retrieval, preprocessing, and comparison to priori model results (including statistics and plots); inverse modeling setup, procedures and results; posteriori analysis of NO<sub>x</sub> emissions and chemical conditions.

## **Executive Summary**

At the beginning of the project, an Executive Summary will be submitted to the Project Manager for use on the AQRP website. The Executive Summary will provide a brief description of the planned project activities, and will be written for a non-technical audience.

Due Date: Friday, January 9, 2015

## **Quarterly Reports**

The Quarterly Report will provide a summary of the project status for each reporting period. It will be submitted to the Project Manager as a Word doc file. It will not exceed 2 pages and will be text only. No cover page is required. This document will be inserted into an AQRP compiled report to the TCEQ.

Due Dates:

Report	Period Covered	Due Date
Quarterly Report #1	January, February 2015	Friday, February 27, 2015
Quarterly Report #2	March, April, May, 2015	Friday, May 29, 2015
Quarterly Report #3	June, July, August, 2015	Monday, August 31, 2015
Quarterly Report #4	September, October, November, 2015	Monday, November 30, 2015

### Technical Reports

Technical Reports will be submitted monthly to the Project Manager and TCEQ Liaison as a Word doc using the AQRP FY14-15 MTR Template found on the AQRP website.

Due Dates:

Report	Period Covered	Due Date
Technical Report #1	Project Start – February 28, 2015	Monday, March 9, 2015
Technical Report #2	March 1 - 31, 2015	Wednesday, April 8, 2015
Technical Report #3	April 1 - 28, 2015	Friday, May 8, 2015
Technical Report #4	May 1 - 31, 2015	Monday, June 8, 2015
Technical Report #5	June 1 - 30, 2015	Wednesday, July 8, 2015
Technical Report #6	July 1 - 31, 2015	Monday, August 10, 2015
Technical Report #7	August 1 - 31, 2015	Tuesday, September 8, 2015

### Financial Status Reports

Financial Status Reports will be submitted monthly to the AQRP Grant Manager (Maria Stanzone) by each institution on the project using the AQRP FY14-15 FSR Template found on the AQRP website.

Due Dates:

Report	Period Covered	Due Date
FSR #1	Project Start – February 28, 2015	Monday, March 16, 2015
FSR #2	March 1 - 31, 2015	Wednesday, April 15, 2015
FSR #3	April 1 - 28, 2015	Friday, May 15, 2015
FSR #4	May 1 - 31, 2015	Monday, June 15, 2015
FSR #5	June 1 - 30, 2015	Wednesday, July 15, 2015
FSR #6	July 1 - 31, 2015	Monday, August 17, 2015
FSR #7	August 1 - 31, 2015	Tuesday, September 15, 2015
FSR #8	September 1 - 30, 2015	Thursday, October 15, 2015
FSR #9	Final FSR	Monday, November 16, 2015

### **Draft Final Report**

A Draft Final Report will be submitted to the Project Manager and the TCEQ Liaison. It will include an Executive Summary. It will be written in third person and will follow the State of Texas accessibility requirements as set forth by the Texas State Department of Information Resources.

Due Date: Tuesday, August 18, 2015

### **Final Report**

A Final Report incorporating comments from the AQRP and TCEQ review of the Draft Final Report will be submitted to the Project Manager and the TCEQ Liaison. It will be written in third person and will follow the State of Texas accessibility requirements as set forth by the Texas State Department of Information Resources.

Due Date: Wednesday, September 30, 2015

### **Project Data**

All project data including but not limited to QA/QC measurement data, databases, modeling inputs and outputs, etc., will be submitted to the AQRP Project Manager within 30 days of project completion. The data will be submitted in a format that will allow AQRP or TCEQ or other outside parties to utilize the information.

### **AQRP Workshop**

A representative from the project will present at the AQRP Workshop in June 2015.

## 2.4 Project Timeline

The following table describes the project timeline.

Task	Jan.- March 2015	March- April 2015	April- May 2015	June- Sep. 2015
<b>Task 1: WRF and CMAQ modelings</b>				
Setup an objective analysis and run WRF with the objective analysis (Dr. Xiangshang Li)	■			
Perform WRF and CMAQ simulations (Ph.D. student, Lijun Diao and Dr. Xiangshang Li)	■			
<b>Task 2: Compare model to satellite NO<sub>x</sub> data</b>				
Data access and data preprocessing (Ph.D. student, Amir Souri)		■		
Compare satellite data to model output (Ph.D. student, Amir Souri)		■		
<b>Task 3: Compare model to aircraft and surface data</b>				
Data access and data preprocessing (Dr. Xiangshang Li)			■	
Compare aircraft and surface monitor data to model output (Dr. Xiangshang Li)			■	
<b>Task 4: Inverse modeling</b>				
Setup an inverse modeling system (Dr. Yunsoo Choi and Ph.D. student, Amir Hossein Souri)			■	
Apply for the inverse model to get posteriori NO <sub>x</sub> source (Ph.D. student, Amir Hossein Souri)			■	
Run the CMAQ runs with the posteriori emissions (Ph.D. students, Amir Hossein Souri and Lijun Diao)				■
<b>Task 5: Evaluate of emission uncertainty on O<sub>3</sub> chemistry</b>				
Estimate NO <sub>2</sub> /HCHO ratio over the Southeast Texas (Ph.D. student, Amir Souri)				■
Estimate the impact of the emission changes on O <sub>3</sub> and NO <sub>x</sub> (Ph.D. student, Lijun Diao and Dr. Xiangshang Li)				■

### 3.0 References

- Atkinson, R. and Arey, J., 1998, Atmospheric Chemistry of Biogenic Organic Compounds, *Acc. Chem. Res.*, 31, 574-583
- Allen, D.J., Pickering, K.E., Pinder, R.W., Henderson, B.H., Appel, K.W., and Prados, A., 2012, Impact of lightning-NO on eastern United States photochemistry during the summer of 2006 as determined using the CMAQ model, *Atmos. Chem. Phys.*, 12, 1737-1785
- Banta, R.M., Senff, C.J., Nielsen-Gammon, J., Darby, L.S., Ryerson, T.B., Alvarez, R.J., Sandberg, S.R., Williams, E.J., Trainer, M., 2005. A bad air day in Houston. *Bulletin of the American Meteorological Society* 86, 657-669.
- Bucsela, E. J., et al. 2013. A new stratospheric and tropospheric NO<sub>2</sub> retrieval algorithm for nadir-viewing satellite instruments: application to OMI. *Atmos. Meas. Tech.*, 6, 2607-2626, doi:10.5194/amt-6-2607-2013
- Choi, Y., Wang, Y., Zeng, T., Martin, R.V., Kurosu, T.P., Chance, K., 2005, Evidence of lightning NO<sub>x</sub> and convective transport of pollutants in satellite observations over North America. *Geophys. Res. Lett.*, 32, L02805, doi:10.1029/2004GL021436
- Choi, Y., Wang, Y., Zeng, T., Cunnold, D., Yang, E., Martin, R., Chance, K., Thouret, V., Edgerton, E., 2008a. Springtime transition of NO<sub>2</sub>, CO and O<sub>3</sub> over North America: Model evaluation and analysis, *Journal of Geophysical Research*, 113, D20311, doi:10.1029/2007JD009632
- Choi, Y., Wang, Y., Yang, Q., Cunnold, D., Zeng, T., Shim, C., Luo, M., Eldering, A., Bucsela, E., Gleason, J., 2008b, Spring to summer northward migration of high O<sub>3</sub> over the western North Atlantic, 2008b, *Geophys. Res. Lett.*, 35, L04818, doi:10.1029/2007GL032276
- Choi, Y., Kim, J., Eldering, A., Osterman, G., Yung, Y.L., Gu, Y., Liou, K.N., 2009, Lightning and anthropogenic NO<sub>x</sub> sources over the United States and the western north Atlantic Ocean: impact on OLR and radiative effects. *Geophys. Res. Lett.*, 36, L17806, doi:10.1029/2009GL039381
- Choi, Y., Osterman, G., Eldering A., Wang, Y., and Edgerton, E., 2010, Understanding the contributions of anthropogenic and biogenic sources to CO enhancements and outflow observed over North America and the western Atlantic Ocean by TES and MOPITT, *Atmospheric Environment*, 44, 2033-2042
- Choi, Y., Kim, H., Tong, D., and Lee, P., Summertime weekly cycles of observed and modeled NO<sub>x</sub> and O<sub>3</sub> concentrations as a function of satellite-derived ozone production sensitivity and land use types over the Continental United States, 2012, *Atmos. Chem. Phys.*, 6291-6307.

Choi, Y., The impact of satellite-adjusted NO<sub>x</sub> emissions on simulated NO<sub>x</sub> and O<sub>3</sub> discrepancies in the urban and outflow areas of the Pacific and Lower Middle US, 2014, *Atmos. Chem. Phys.*, 14, 675-690

Czader, B.H., Li, X.S., Rappenglueck, B., 2013. CMAQ modeling and analysis of radicals, radical precursors, and chemical transformations. *J Geophys Res-Atmos* 118, 11376-11387.

Czader, B., Choi, Y., Li, X., Alvarez, S., and Lefer, B., 2014, Impact of updated traffic emissions on HONO mixing ratios simulated for urban site in Houston, Texas, *Atmos. Chem. Phys. Discuss.*, 14, 21315-21340

Duncan, B.N., Yoshida, Y., Olson, J.R., Silman, S., Martin, R.V., Lamsal, L., Hu, Y., Pickering, K.E., Retscher, C., Allen, D.J., Crawford, J.H., 2010, Application of OMI observations to a space-based indicator of NO<sub>x</sub> and VOC controls on surface ozone formation, *Atmospheric Environment*, 44(18), 2213-2223.

Duncan, B.N, et al. (2014). Satellite data of atmospheric pollution for U.S. air quality applications: Examples of applications, summary of data end-user resources, answers to FAQs, and common mistakes to avoid, *Atmospheric Environment*, 94:647-662, doi:10.1016/j.atmosenv.2014.05.061.

Guenther, A., Hewitt, C.N., Erickson, D., Fall, R., Geron, C., Graedel, T., Harley, P., Klinger, L., Lerdau, M., McKay, W.A., Pierce, T., Scholes, B., Steinbrecher, R., Tallamraju, R., Taylor, J., and Zimmerman, P., 1995, A global model of natural volatile organic compound emissions, *J. Geophys. Res.*, 100, D5, 8873-8892

Guenther, A., Baugh, B., Brasseur, G., Greenberg, J., Harley, P., Klinger, L., Serca, D., and Vierling, L., 1999, Isoprene emission estimates and uncertainties for the Central African EXPRESSO study domain, *J. Geophys. Res.*, 104, D23, 30625-30639

Houyoux, M.R., Vulkovich, J.M., Coats, C.J., Wheeler, N.M., and Kasibhatla, P.S., 2000, Emission inventory development and processing for the Seasonal Model for Regional Air Quality (SMRAQ) project, *J. Geophys. Res.*, 105, 9079-9090

Hudman, R.C., Murray, L.T., Jacob, D.J., Millet, D.B., Turquety, S., Wu, S., Blake, D.R., Goldstein, A.H., Holloway, J., and Sachse, G.W., 2009, Biogenic versus anthropogenic sources of CO in the United States, *Geophys. Res. Lett.*, 35, L04801, doi:10.1029/2007GL032393

Kuhlmann, G., Hartl, A., Cheung, H. M., Lam, Y. F., and Wenig, M. O.: A novel gridding algorithm to create regional trace gas maps from satellite observations, *Atmos. Meas. Tech.*, 7, 451-467, doi:10.5194/amt-7-451-2014, 2014.

Li, X., Choi, Y., Czader, B., Kim, H., 2014. The impact of the observation nudging and nesting on the simulated meteorology and ozone concentrations from WRF-SMOKE-CMAQ during DISCOVER-AQ 2013 Texas campaign. To be submitted.

- Martin, R.V., Fiore, A.M., and Donkelaar, A.V., Space-based diagnosis of surface ozone sensitivity to anthropogenic emissions, 2004, *Geophys. Res. Lett.*, 31, L06120, doi:10.1029/2004GL019416
- Millet, D.B., Goldstein, A.H., Holzinger, R., Williams, B.J., Allan, J.D., Jimenez, J.L., Worsnop, D.R., Roberts, J.M., White, A.B., Hudman, R.C., Bertschi, I.T., Stohl, A., 2006, Chemical characteristics of north American surface layer outflow: insights from Chebogue point, Nova Scotia, *J. Geophys. Res.*, 111, D23S53
- Ngan, F., Byun, D., Kim, H., Lee, D., Rappengluck, B., Pour-Biazar, A., 2012. Performance assessment of retrospective meteorological inputs for use in air quality modeling during TexAQS 2006. *Atmos. Env.* 54, 86-96.
- Palmer, P.I., Jacob, D.J., Fiore, A.M., Martin, R.V., Chance, K., and Kurosu, T.P., Mapping isoprene emissions over North America using formaldehyde column observations from space, 2003, 108, D6, 4180, doi:10.1029/2002JD002153
- Pfister, G.G., Emmons, L.K., Hess, P.G., Lamarque, J.-F., Orlando, J.-J., Walters, S., Guenther, A., Palmer, P., Lawrence, P.J., 2008, Contribution of isoprene to chemical budgets: a model tracer study with the NCAR CTM MOZART-4, *J. Geophys. Res.*, 113, D05308
- Rappenglück, B., B. Lefer, B. Czader, X. Li, J. Golovko, S. Alvarez, J. Flynn, C. Haman, and N. Grossberg. 2011. University of Houston Moody Tower 2010 Ozone Formation Research Monitoring; Project Grant No. 582-5-64594-FY10-14, Prepared for the Texas Commission on Environmental Quality, TX 2011
- Rodgers, C.D., *Inverse Methods for Atmospheric Sounding: Theory and Practice*, 2000, World Sci., Hackensack, N.J.
- Russell, A. R., Perring, A. E., Valin, L. C., Bucsela, E. J., Browne, E. C., Wooldridge, P. J., and Cohen, R. C. (2011). A high spatial resolution retrieval of NO<sub>2</sub> column densities from OMI: method and evaluation. *Atmos. Chem. Phys.*, 11, 8543-8554, doi:10.5194/acp-11-8543-2011.
- Sharkey, T.D., Singaas, E.L., Lerdau, T., Geon, C.D., 1999, Weather effects on isoprene emission capacity and applications in emissions in emission algorithms, *Ecological Applications*, 9, 1131-1137
- Shim, C., Wang, Y., Choi, Y., Palmer, P.I., Abbot, D.S., and Chance, K., Constraining global isoprene emissions with Global Ozone Monitoring Experiment (GOME) formaldehyde column measurements, *J. Geophys. Res.*, 110, D24301, doi:10.1029/2004JD005629
- Zhao, C., Wang, Y., Choi, Y., and Zeng, T., Summertime impact of convective transport and lightning NO<sub>x</sub> production over North America: modeling dependence on meteorological simulations, 2009, *Atmos. Chem. Phys.*, 9, 4315-4327.